TISSUE ENGINEERING: Part C
Volume 22, Number 5, 2016

DOI: 10.1089/ten.tec.2015.0581

termis
Tissue Engineering
& Regenerative Medicine
International Society

METHODS ARTICLE

Surface Chemistry and Microtopography of Parylene C Films Control the Morphology and Microtubule Density of Cardiac Myocytes

Tatiana Trantidou, PhD,[1,2] Eleanor J. Humphrey, MRes,[3] Claire Poulet, PhD,[3] Julia Gorelik, PhD,[3] Themistoklis Prodromakis, PhD,[1,2] and Cesare M. Terracciano, MD, PhD[3]

Cell micropatterning has certainly proved to improve the morphological and physiological properties of cardiomyocytes *in vitro*; however, there is little knowledge on the single cell–scaffold interactions that influence the cells' development and differentiation in culture. In this study, we employ hydrophobic/hydrophilic micropatterned Parylene C thin films (2–10 μm) as cell microscaffolds that can control the morphology and microtubule density of neonatal rat ventricular myocytes (NRVM) by regulating their adhesion area on Parylene through a thickness-dependent hydrophobicity. Structured NRVM on thin films tend to bridge across the hydrophobic areas, demonstrating a more spread-out shape and sparser microtubule organization, while cells on thicker films adopt a cylindrical (*in vivo*-like) shape (contact angles at the level of the nucleus are 64.51° and 84.73°, respectively) and a significantly ($p < 0.05$) denser microtubule structure. Ion scanning microscopy on NRVM revealed that cells on thicker membranes were significantly ($p < 0.05$) smaller in volume, but more elongated. The cylindrical shape and a significantly denser microtubule structure indicate the ability to influence cardiomyocyte phenotype using patterning and manipulation of hydrophilicity. These combined bioengineering strategies are promising tools in the generation of more representative cardiomyocytes in culture.

Introduction

THE ULTIMATE GOAL of any tissue engineering strategy is to produce reliable *in vitro* cell models with application in drug development, disease modeling, and eventually engineered patient-specific organs. Over the last 40 years, researchers in the field of cardiac tissue engineering have experimented with neonatal and embryonic cardiomyocytes of animal origin toward improving their morphological and physiological properties *in vitro* to reconstitute adult cardiac tissue level functionality. The main goal of these efforts was to fully understand the mechanisms by which cells in culture interact with their scaffold and how these affect their development and differentiation.

Among different approaches, cell patterning induces the alignment and elongation of immature cardiac myocytes, improving many morphological and physiological properties of cardiac tissue, such as sarcomere organization,[1] Ca^{2+} handling,[1–3] gap junction protein (connexin43) expression,[4] and directionality of action potential propagation.[5–9]

Several different methodologies have been developed for cardiac tissue engineering using neonatal rat ventricular myocytes (NRVM)[2,5–9] and induced pluripotent stem cell-derived cardiomyocytes.[1] These techniques include microcontact printing of substrates with extracellular matrix (ECM) compounds,[5] deposition of ECM proteins and cells through microfluidic channels,[10] microgrooved substrates,[1,5,6,8,9] nanotextured hydrogels,[11] and lithographically patterned substrates.[2,7] Structured cardiomyocyte cultures have also been realized in three dimensions with the use of naturally or synthetically produced ECMs produced through electrospinning of aligned polymer nanofibers[12] and production of macroporous preformed scaffolds with complex biomimetic pore structures.[13]

Our group has previously developed a reliable and reproducible scaffolding technology using Parylene C thin films, which were micropatterned through selective modification of the material's inherent hydrophobicity using standard lithography and oxygen plasma.[2] These polymer scaffolds were able to align NRVM and significantly ($p < 0.05$) improve

[1]Centre for Bio-Inspired Technology, Imperial College London, London, United Kingdom.
[2]Nano Group, ECS, University of Southampton, Southampton, United Kingdom.
[3]National Heart and Lung Institute, Imperial College London, London, United Kingdom.

their immature Ca^{2+} transients at 0.5–2 Hz field stimulation. This scaffolding technology also enabled the production of structured NRVM cultures on planar Multi Electrode Arrays, which had an improved action potential conduction velocity and anisotropy.[14]

Parylene C is a highly biocompatible material, which has a long history of use in the field of medical implants and microdevices, such as pacemakers,[15] sensors,[16] and microelectrodes.[17] Besides biocompatibility, the material has been widely used for encapsulation due to its excellent electrical, thermal, and physical properties. These inherent properties, however, are thickness dependent,[18–20] which is attributed to a transition from an amorphous to a semicrystalline structure as thickness increases.[18] In fact, we have previously demonstrated that Parylene C exhibits a thickness-dependent hydrophobicity, with thicker films being more hydrophobic than thinner films.[21]

In this study, we hypothesize that certain morphological parameters of structured cardiac myocytes on micropatterned Parylene C films can be further manipulated by controlling the film thickness and thus the degree of surface hydrophobicity. To test the hypothesis, we cultured NRVM on glass substrates coated with 2 and 10 μm-thick Parylene C films, which were selectively plasma oxidized to create local hydrophilic areas for cell attachment. In addition to Ca^{2+} transients, we studied cellular morphology, adhesion area, and microtubule density to investigate the effect of the substrate hydrophobicity on cellular morphology and physiology.

Materials and Methods

Fabrication of the microengineered Parylene C constructs

The fabrication process has been previously presented.[12] Briefly, standard glass coverslips (0.15 mm thick) of 13 mm in diameter (VWR) were cleaned in acetone, isopropanol (all Sigma-Aldrich), and deionized (DI) water, and dehydrated on a hotplate at 90°C for 60 s. Parylene C films of 2 and 10 μm thickness were deposited by chemical vapor deposition using a commercially available coater (PDS2010, SCS). Hexamethyldisilazane (Sigma-Aldrich) was spin coated on the Parylene C-coated coverslips, succeeded by a 1.4 μm thick positive photoresist (AZ5214, Microchemicals GmbH). The samples were then soft baked on a hotplate at 90°C for 60 s, selectively exposed to ultraviolet light (Karl Suss MA6) through a chrome-plated glass mask, comprising transparent areas of 10 μm equally spaced parallel lines. The samples were developed in 4:1 DI water:AZ400k (Microchemicals GmbH). The samples were prebaked on a hotplate at 110°C for 60 s. Selective hydrophilic patterning was achieved through plasma oxidation using a plasma etcher (Nano UHP LFG40, Diener electronic) at 400 W/5 min, 0.8 mbar working pressure, and frequency of 13.56 MHz. After plasma oxidation, the remaining photoresist was removed through immersion in acetone. The resulting surface layout of the Parylene C substrates had parallel hydrophobic-hydrophilic lines 10 μm wide (Fig. 1A). The dimensions of the pattern—equally spaced (10 μm) 10 μm-wide parallel lines—were determined based on previous studies with NRVM, suggesting that lines of this width most effectively align the cardiomyocytes and elongate their nuclei, while maintaining a confluent monolayer of cells.[1,2] Parylene C-coated coverslips that were plasma oxidized under the same conditions (400 W/5 min) were used as the control (unpatterned) group.

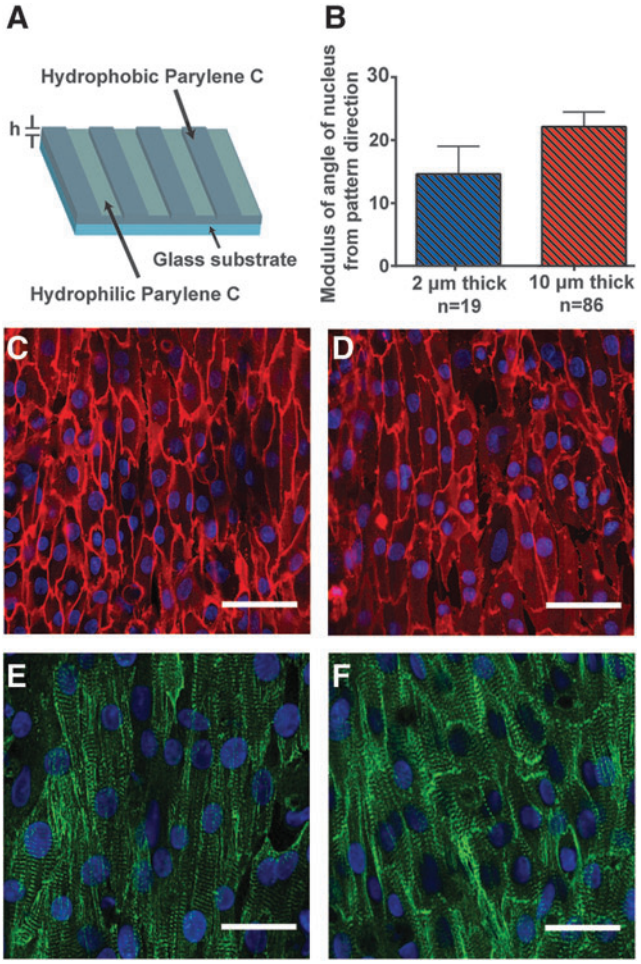

FIG. 1. Neonatal rat ventricular myocytes (NRVM) on the microengineered Parylene C constructs. **(A)** Schematic representation of the fabrication process of the microengineered constructs. *h* represents the Parylene C film thickness. **(B)** Quantification of NRVM alignment on 2 μm-thick (*blue*) and 10 μm-thick (*red*) micropatterned Parylene C surfaces. *n* represents the number of cells. Data derived from two isolations. Error bars indicate standard error of mean (SEM). Representative immunofluorescence of NRVM cultured on **(C, E)** 2 μm-thick and **(D, F)** 10 μm-thick Parylene C constructs. *Red*, membrane stain cell mask *orange*. *Green*- alpha sarcomeric actinin antibody. *Blue*, nuclear stain Hoechst 33258 in **(C, D)** and DAPI in **(E, F)**. Bars-50 μm in **(C, D)** and 30 μm in **(E, F)**. Color images available online at www.liebertpub.com/tec

Cardiomyocyte isolation and culture

All experiments were conducted in accordance with Home Office regulations detailed in the Animals (Scientific Procedures) Act 1986 and the EU Directive 2010/63/EU. All experimental protocols were approved by the Central Biomedical Science unit, Imperial College London. Cervical dislocation was performed with a pause afterward, followed by confirmation of permanent cessation of the circulation. NRVM were isolated using the GentleMACs Neonatal Heart Dissociation Kit (Mi Kit, Miltenyi Biotec GmbH). Briefly, the preparation steps include the reagent preparation step 1

using medium-199 (Corning), the dissociation protocol step 1 using Hank's balanced salt solution (HBSS; Sigma-Aldrich), the dissociation protocol steps 11–13 using medium-199 supplemented with 10% neonatal calf serum, 50 U/mL penicillin (Sigma-Aldrich), 2 mg/mL vitamin B12, and 200 mM L glutamine, the dissociation protocol step 14, and centrifugation at 1000 rpm, for 5 min. The solution was resuspended in 20 mL supplemented medium-199 and preplated for 1 h to remove fibroblasts. The cells were then counted using a hemocytometer. Before seeding, constructs were sterilized by double submersion in 70% ethanol for 10 min. The samples were left to dry in a sterile environment and subsequently washed twice with sterile phosphate-buffered saline (PBS; Oxoid) and then with sterile DI water to remove any crystal compounds from the surface. After drying out, the constructs were coated with 5 mg of type IV human placenta collagen (Sigma-Aldrich) diluted in 22 mL of HBSS and 3 mL of glacial acid. The solution was applied on the constructs for 1 min and was succeeded with two quick washes with sterile DI water. Finally, the constructs were immersed into water and stored for 1 h in the incubator (37°C, 5% CO_2). Before seeding, water was removed. 50×10^3 cells in 10 μL medium consisting of 67% Dulbecco's modified Eagle's medium (DMEM; Gibco), 16% medium-199, 10% horse serum (Sigma-Aldrich), 4% fetal bovine serum (Sigma-Aldrich), 2% 1 M HEPES (Sigma-Aldrich), and 1% penicillin-streptomycin (Sigma-Aldrich) were seeded on each construct. All constructs were then incubated for half an hour to allow the cells to attach on the surface. Subsequently, the container plate was gently filled with the cell medium (500 μL). Complete medium was changed 18 h after seeding. All experiments were performed at day 4 postseeding.

Immunofluorescence

To determine cell alignment, the cellular plasma membranes of live NRVM were labeled with 1.6 mM di-8-ANEPPS (Invitrogen), which has been shown in multiple studies to preserve the sophisticated function of cardiac myocytes. The nuclear deoxyribonucleic acid of the cells was labeled with Hoechst 33258 (H258; Invitrogen). The constructs were incubated with 12.5 μL of di-8-ANEPPs and 0.5 μL of H258 prepared in 0.5 mL DMEM for 5 min at 37°C and 5% CO_2.

In some cases, to avoid internalization of di-8-ANEPPS within the cell, plasma membranes were stained with cell mask orange (1:500 dilution; Invitrogen). The constructs were incubated with the dye solution prepared in DMEM for 10 min at 37°C and then washed thrice in HBSS.

Staining of the NRVM sarcomeres was performed using alpha sarcomeric actinin (Sigma-Aldrich) as the primary antibody. The cells were fixed with cold acetone (Sigma-Aldrich) for 10 min, washed five times with PBS (10 min each), and blocked with 1% bovine serum albumin (BSA) and 0.1% triton in PBS solution for 1 h at room temperature. Subsequently, the cells were incubated with the primary antibody (concentration 1:80) for 3 h, then washed thrice with PBS for 15 min, and finally incubated with the secondary antibody Alexa 488 (Invitrogen) for 1.5 h. Finally, cells were washed with PBS and mounted with the DAPI (Invitrogen) medium.

To quantify the density and organization of the microtubules, NRVM were stained for α-tubulin. Cells were washed in PBS, fixed with ice-cold methanol for 5 min, and blocked in 1% BSA prepared in PBS (which was subsequently used for all antibody dilutions) for 1 h to prevent nonspecific binding. Cells were stained with a mouse anti-α tubulin antibody (1:500 dilution; Sigma-Aldrich) overnight at 4°C and then incubated with an anti-mouse Alexa 488 antibody (1:500 dilution; Millipore) for 1 h before mounting using a vectashield (Vector Labs) mounting medium containing DAPI (Invitrogen). The cells were imaged under an inverted Zeiss LSM-780 confocal microscope. All immunofluorescence experiments were conducted at day 4 postseeding.

Assessment of alignment and elongation

Cell alignment was assessed based on nuclear alignment angles, defined as the orientation of the major elliptic axis of individual nuclei with respect to the direction of the patterning. Nuclear alignment angles were measured using built-in functions of a dedicated image processing software tool (Fiji, NIH). Cardiomyocyte elongation was quantified by calculating the aspect ratio of the major to the minor axis of the cell's nucleus.

Assessment of contact angles

To assess the position and morphology of the cells on the micropatterned constructs, z-stack images of the cells on the Parylene C surfaces were taken using the confocal microscope at a depth of 1 μm per slice and then reconstructed using image analysis software (Fiji, NIH). Images were obtained at a 512×512 resolution, which was determined to be a good balance between image quality and acquisition time. The volumetric affinity of the cells to their culture substrate was investigated through contact angle measurements at the level of the nucleus based on the orthogonal views of the acquired confocal images. Contact angle was measured thrice from the base of the cell to the edge of the plasma membrane and the average value was taken for each case.

Assessment of microtubule density

To quantify the microtubule density, analysis of the images was performed using dedicated image processing software (Fiji, NIH). The background was subtracted from the image and a rectangular area (30×60 pixels) was selected within a cell. A threshold was applied to the selection, and the percentage area covered by microtubules was measured.

Measurement of Ca^{2+} transients

Ca^{2+} experiments for NRVM were performed using optical mapping and an inverted Zeiss fluorescent microscope. NRVM were loaded with 500 μL HBSS and 5 μL of a solution consisting of 50 μg fluo-4-AM diluted in 50 μL pluronic F-127 (20% solution in dimethyl sulfoxide—DMSO; Invitrogen). The cells were then placed in the incubator for 15 min and then de-esterified with 500 μL HBSS for 20 min. During the experiments, cells were superfused with 37°C Normal Tyrode's solution containing 140 Mm NaCl, 6 mM KCl, 1 mM $MgCl_2$, 1 mM $CaCl_2$, 10 mM glucose, and 10 mM HEPES adjusted to pH 7.4 with 2 M NaOH (all Sigma-Aldrich). The Ca^{2+} transients were studied using 20× magnification under 0.5, 1, and 2 Hz field stimulation to induce rhythmic

depolarization. Ca^{2+} transients were collected through a dedicated software (IDL; Research Systems, Inc.) and analyzed by an automated procedure performed in MATLAB® to calculate amplitude (f/f0), time to peak (Tp), time to 50% (T50), and time to 90% (T90) decline.

Hopping probe ion conductance microscopy

Hopping probe ion conductance microscopy (HPICM) is a variant of Scanning Ion Conductance Microscopy, in which ion current through a fluid-filled nanopipette is a function of the distance between the pipette tip and the surface.[22] A nanopipette containing a silver electrode is mounted on a three-dimensional piezoelectric translation stage (Physik Instrumente) and ion flow through the pipette is measured using an Axopatch 200A amplifier (Molecular Devices). A change in the current sends a feedback signal to readjust the vertical position of the pipette, thereby maintaining a constant distance between the pipette and the surface. A topographical image is then generated by measuring the movement of the pipette in the z direction, while a sample is scanned in the x and y directions.[23] Glass nanopipettes of $\sim 90\,m\Omega$ resistance were pulled from borosilicate capillaries and filled with the following solution (in mM): NaCl 144, KCl 5, $MgCl_2$ 1, HEPES 10.

Statistical analysis

Statistical analysis was performed using an unpaired t-test (two-tailed) with a confidence interval of 95%. Data are expressed as mean ± standard error of mean unless specified otherwise. For the cell alignment, contact angle, and HPICM studies, n represents the number of cells. For the Ca^{2+} cycling studies, n represents the number of constructs. In the Figures, *indicates $p<0.05$; **$p<0.01$; and ***$p<0.001$. The analysis was performed using Prism 4 software (GraphPad software, Inc.).

Results

Cell alignment and sarcomere structure

NRVM were cultured on micropatterned Parylene C films of 2 and 10 μm thickness (Fig. 1A). In both cases, an aligned confluent monolayer of cells was achieved, with the cells being elongated along the direction of the micropatterned lines. Cell alignment was quantified based on the angle between the long axis of the cell nucleus and the direction of lines. No statistically significant difference in the alignment of NRVM was observed between 2 and 10 μm thick Parylene C films, as shown in Figure 1B [average values of NRVM on 2 μm thick films was 14.59° ($n=19$ cells) and for 10 μm thick films was 22.12° ($n=86$ cells)].

Figure 1C, D show representative immunofluorescence images of NRVM cultured on micropatterned Parylene C films of 2 and 10 μm thickness, respectively. The sarcomeric structures of the NRVM on the thin (Fig. 1E) and thick (Fig. 1F) micropatterned Parylene C films were equally organized, as seen in the aligned α-actinin striation pattern of the myofibrils. Evaluation of sarcomeric length on NRVM did not reveal any significant differences between cultures on the thin and thick micropatterned Parylene C films (Supplementary Fig. S1; Supplementary Data are available online at www.liebertpub.com/tec).

Calcium cycling

We have previously demonstrated that the Ca^{2+} cycling of NRVM cultured on micropatterned Parylene C films (1–10 μm) is significantly improved compared to NRVM cultured on conformally oxygen plasma-treated (hydrophilic) Parylene C films of same thickness.[2] In particular, we examined normalized fluorescent amplitude (f/f0), time to transient peak (Tp), time to 50% transient decay (T50), and time to 90% transient decay (T90), which were all significantly affected at 0.5, 1, and 2 Hz field stimulation.

In this study, we field stimulated NRVM cultures on micropatterned 2 and 10 μm-thick films at 0.5, 1, and 2 Hz frequencies and examined their Ca^{2+} handling in terms of f/f0, Tp, T50, and T90. Although there is a clear difference between Ca^{2+} transients of structured and unstructured cells, there were no significant differences between structured cells on thin and thick micropatterned Parylene C films for all four parameters (f/f0, Tp, T50, and T90) at all stimulation frequencies (Supplementary Fig. S2). Table 1 summarizes the corresponding Ca^{2+} cycling data for the two groups at all field stimulation frequencies. Representative Ca^{2+} transients are presented in Supplementary Figure S3.

Cell morphology

To examine how single cells interact with their substrate, cells at the edges of the culture were individually analyzed as these were clearly visible. Figure 2 demonstrates representative immunofluorescence pictures of NRVM seeded on the micropatterned thin and thick constructs together with the corresponding cross-sectional views. Cells on thick (10 μm) membranes were less likely to bridge across the hydrophobic lines and constrained on the hydrophilic lines, maintaining a more cylindrical shape. On the contrary, the majority of cells cultured on thin membranes managed to cross the hydrophobic lines and adhere to the two adjacent hydrophilic lines, obtaining a more spread-out shape.

Figure 3A, B summarize these observations by presenting a simple schematic of the position of cells on the micropatterned Parylene C constructs. The corresponding statistical

Table 1. CA^{2+} Transient Data from NRVM Cultured on 2 and 10 μm-Thick Micropatterned Parylene C Constructs (mean ± SD)

Stimulation frequency	*Parameter*	*2 μm-thick parylene C*	*10 μm-thick parylene C*
0.5 Hz	F/F0	4.228 ± 1.254	4.140 ± 1.218
	Tp	117.2 ± 27.78	121.9 ± 24.61
	T50	251.3 ± 87.78	244.0 ± 80.32
	T90	796.8 ± 200.6	778.3 ± 190.4
1 Hz	F/F0	3.530 ± 1.058	3.799 ± 0.957
	Tp	114.4 ± 36.56	108.5 ± 12.98
	T50	203.5 ± 77.65	203.6 ± 58.49
	T90	508.8 ± 120.3	508.2 ± 118.3
2 Hz	F/F0	2.764 ± 0.716	2.826 ± 0.765
	Tp	96.66 ± 28.37	96.19 ± 23.02
	T50	153.1 ± 26.74	155.4 ± 26.74
	T90	309.9 ± 31.33	308.9 ± 37.40

Data derived from $n=13$ constructs and seven isolations.
NRVM, neonatal rat ventricular myocytes.

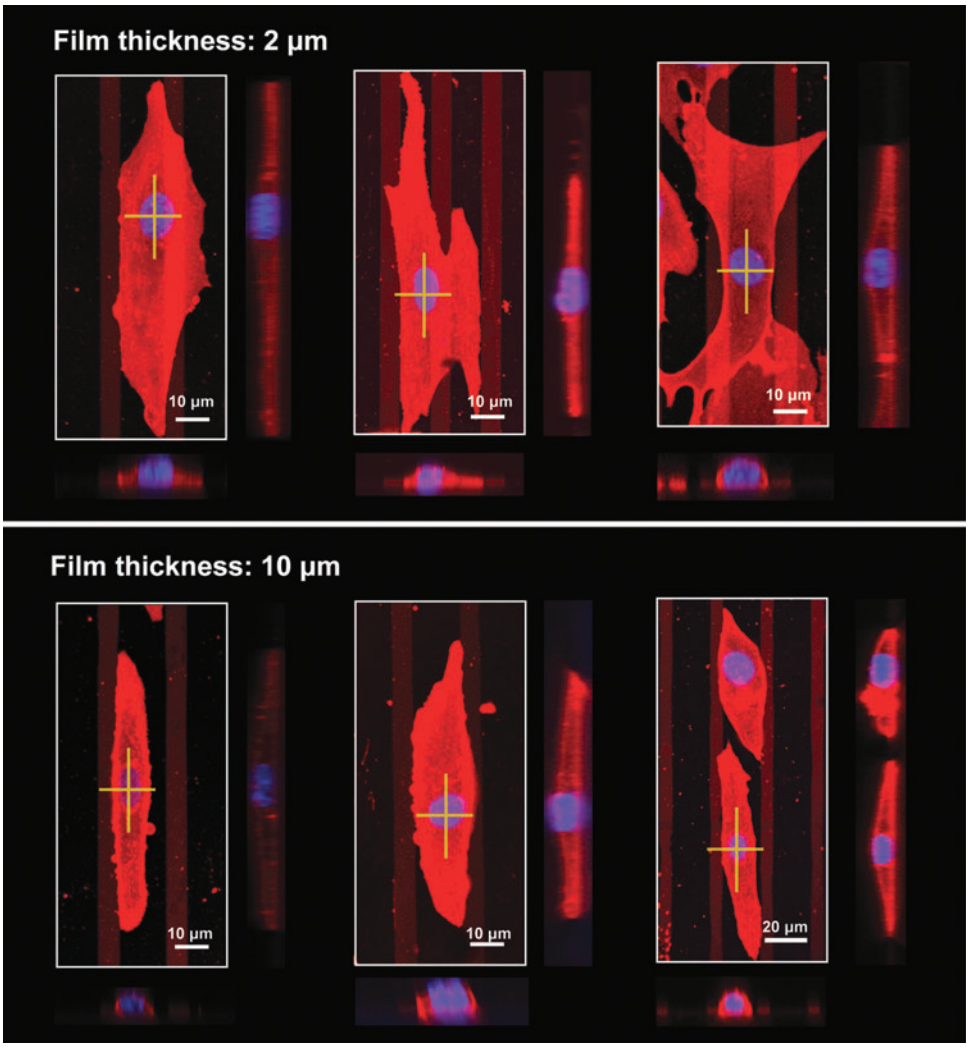

FIG. 2. Representative immunofluorescence images and cross-sectional views (taken from the corresponding crosses) of NRVM. Cells are cultured on 2 μm-thick (*top*) and 10 μm-thick (*bottom*) Parylene C micropatterned constructs. *Red*, membrane stain cell mask *orange*. *Blue*, nuclear stain Hoechst 33258. Color images available online at www.liebertpub.com/tec

analysis of the cells' position revealed that 89.58% of the cells examined were able to bridge across the hydrophobic lines on the thin Parylene C constructs ($n=58$ cells), whereas this trend was obvious only for 61.82% of the cells seeded on the thick constructs ($n=55$ cells) (Fig. 3C).

The surface affinity of the cells to their culture substrate was investigated through contact angle measurements at the level of the nucleus based on the orthogonal views of the acquired confocal images. Figure 3D provides the statistical analysis (two-tailed *t*-test unpaired) derived from this study. The contact angle of cells sitting on the thick membranes ($84.73\pm4.9°$, $n=27$ cells) was significantly larger ($p<0.01$) compared to cells cultured on the thin membranes ($64.51\pm5.3°$, $n=25$ cells).

The height, surface, volume, and elongation of live NRVM on the micropatterned constructs were examined using HPICM at nanoscale resolution. Figure 4 shows representative images of NRVM on the thin (Fig. 4A left) and thick (Fig. 4A right) Parylene C constructs, while the corresponding 3-D topographical rendered images of the cells are depicted below.

Elongation index was calculated as the length of the cell divided by its width (an elongation index that equals 1 means that the cell is round). The average elongation index was significantly larger in cells grown on thick membranes (Fig. 4B; cells on thin films: 3.16 ± 0.16, $n=67$ cells; cells on thick films: 3.66 ± 0.20, $n=62$ cells; $p<0.05$). Indeed, a larger fraction of cells on thick constructs had an index above three: 61.3% against 46.3% (Fig. 4C). While cell area was similar between the two groups, cell volume was significantly lower when cells were cultivated on thick membranes (cells on thin films: $2105\pm92\,\mu m^3$, $n=67$ cells; cells on thick films: $1849\pm86\,\mu m^3$, $n=62$ cells; $p<0.05$). Similarly, cell height was significantly lower for cells cultured on thick Parylene films (cells on thin films: 5.96 ± 0.18 μm, $n=67$ cells; cells on thick films: 5.18 ± 0.15 μm, $n=62$ cells; $p=0.001$).

The change in cell morphology observed upon a change in Parylene film thickness is anticipated to relate to changes in the cytoskeletal structure. NRVM cultured on the micropatterned Parylene C constructs were stained for microtubules. As a reference, we also present here two control (unpatterned) groups of Parylene C constructs of same thicknesses (2 and 10 μm) that were conformally plasma oxidized under the same conditions. Figure 5A–D shows representative immunofluorescence images (more images are demonstrated in Supplementary Fig. S4). The greatest number of microtubules was found about the perinuclear region in both the micropatterned

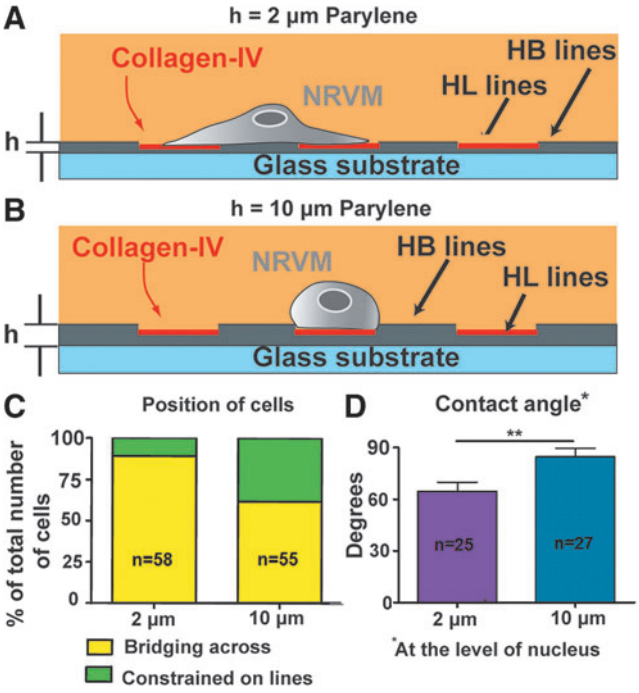

FIG. 3. Morphology and position analysis of cultured NRVM. Schematics showing the position of NRVM on **(A)** the $h = 2\,\mu m$ and **(B)** $h = 10\,\mu m$ thick micropatterned Parylene C substrates. **(C)** Statistics of the cells position on the micropatterned constructs. **(D)** Corresponding contact angle data. Error bars indicate SEM. $^{**}p < 0.01$. n represents the number of cells (Data derived from three isolations). Color images available online at www.liebertpub.com/tec

and unpatterned constructs. Microtubules of structured cells appeared more compact and denser within the cells. On the contrary, microtubules of unstructured cells were more spread out and sparsely distributed throughout the cytoplasm.

Figure 5E summarizes the observations derived from the image analysis. There was a significant increase in the percentage area covered by microtubules for structured cells compared to unstructured cells for both 2 μm-thick films (structured: $63.08\% \pm 1.91\%$, $n = 6$ constructs; unstructured: $55.78\% \pm 1.55\%$, $n = 6$ constructs; $p < 0.05$) and 10 μm-thick films (structured: $68.72\% \pm 1.22\%$, $n = 6$ constructs; unstructured: $54.38\% \pm 0.93\%$, $n = 6$ constructs; $p < 0.001$). It was observed that cells on the 10 μm-thick patterned constructs had a significantly larger microtubule density compared to cells on the 2 μm-thick constructs (structured on 2 μm-thick films: $63.08\% \pm 1.91\%$, $n = 6$ constructs; structured on 10 μm-thick films: $68.72\% \pm 1.22\%$, $n = 6$ constructs; $p < 0.05$). On the contrary, microtubule density did not change between unstructured NRVM cultures on thin and thick membranes.

Discussion

In this study, we demonstrated that the morphology and microtubule density of structured neonatal ventricular cardiomyocytes on hydrophobic/hydrophilic micropatterned Parylene C substrates are controlled by the thickness of the Parylene film due to a thickness-dependent hydrophobicity. Structured cells on thinner (2 μm) micropatterned films obtain a more spread-out shape and have a less dense microtubule organization. On the contrary, structured cells on thicker (10 μm) micropatterned films adopt a smaller, but more elongated shape, while they also have a denser

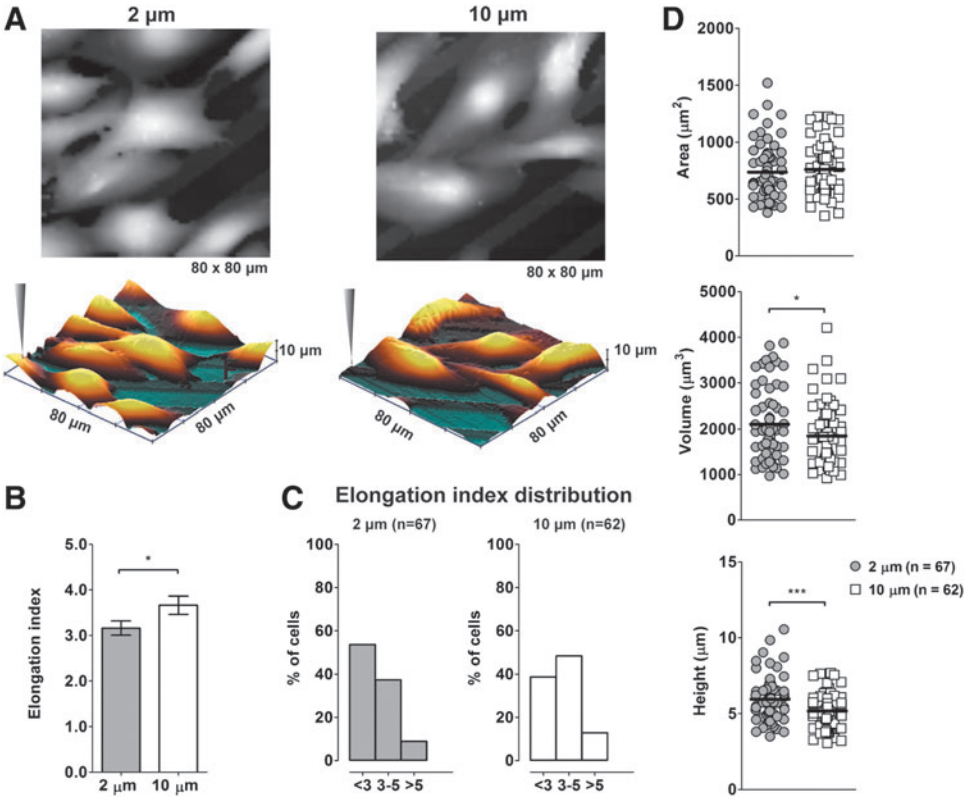

FIG. 4. Topographical images obtained with hopping mode ion conductance microscopy of cultured NRVM. **(A)** Cells are cultured on 2 μm-thick and 10 μm-thick Parylene C constructs. The scanning pipette is depicted in the 3-dimensional reconstruction of the scans. **(B, C)** Elongation index, **(D)** surface, volume, and height of NRVM in relation to film thickness. n represents the number of cells. $^{*}p < 0.05$, $^{***}p < 0.001$ (Data derived from two isolations. Error bars indicate SEM). Color images available online at www.liebertpub.com/tec

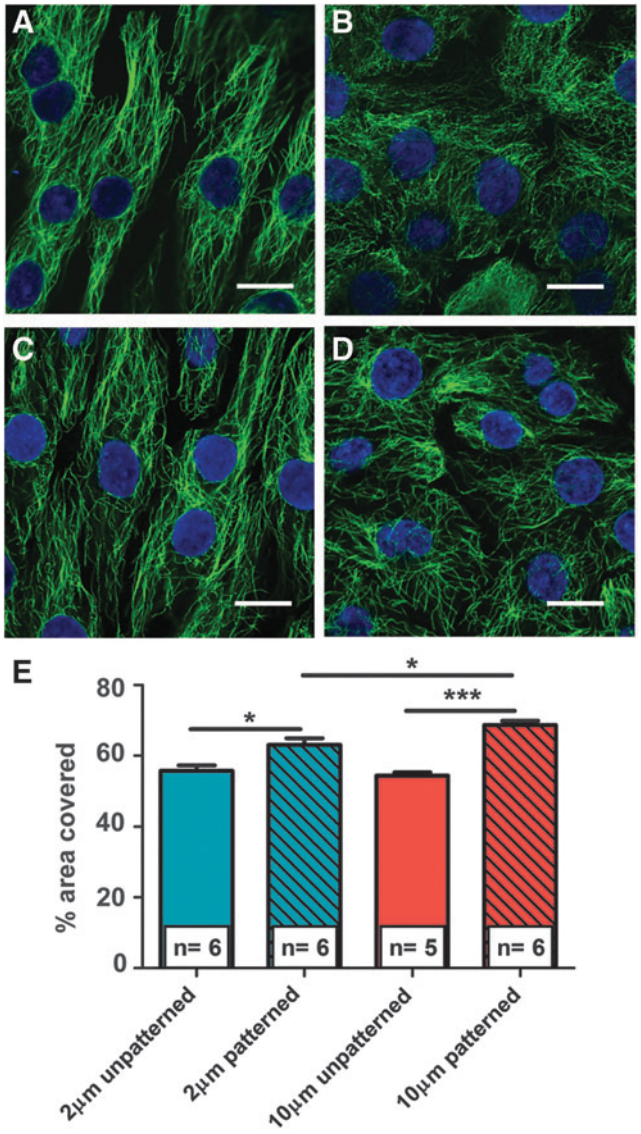

FIG. 5. Representative immunofluorescence images of NRVM stained for microtubules. **(A)** 2 μm-thick patterned substrates, **(B)** 2 μm-thick unpatterned substrates, **(C)** 10 μm-thick patterned substrates, and **(D)** 10 μm-thick unpatterned Parylene C substrates. *Green*, mouse anti α-tubulin antibody. *Blue*, nuclear stain Hoechst 33258. Bars-10 μm in **(A–D)**. **(E)** Quantification of microtubules. *n* represents the number of constructs. $*p < 0.05$, $***p < 0.001$ (Data derived from six isolations. Error bars indicate SEM). Color images available online at www.liebertpub.com/tec

microtubule organization, which closer resembles adult cardiomyocytes. Both the degree of alignment and the Ca^{2+} cycling properties of the cells were unchanged between the two groups. The cylindrical shape and a significantly denser microtubule structure indicate the ability of influencing cardiomyocyte phenotype using patterning and manipulation of hydrophilicity. Combined bioengineering strategies for the manipulation of cell environment are key for the generation of adult-like cardiomyocytes in culture.

There is evidence from other studies to suggest that the water affinity of Parylene C influences cellular morphology. In particular, Chang *et al.*[24] demonstrated that Parylene's natural hydrophobicity causes mouse embryonic fibroblasts (NIH 3T3) to become more raised and rounded in shape compared to those on a conformally plasma-oxidized (hydrophilic) surface. We have previously demonstrated a thickness-dependent surface water affinity of Parylene C thin films ranging from 50 nm to 12 μm thickness.[21] In particular, average contact angles of a 10 μL droplet of DI water on Parylene C-coated glasses were 78.85° for 2 μm-thick films and 88.30° for 10 μm-thick films.

In this study, we exploited this thickness-dependent hydrophobicity to regulate the adhesion area of cardiomyocytes on the Parylene substrate and produce a more representative cellular phenotype. We employed Parylene C films of two distinct thicknesses (2 and 10 μm), as we concluded that the surface hydrophobicity does not significantly change below 2 μm and above 10 μm-film thickness.[21] We selectively changed the material's hydrophobicity, creating sequential hydrophilic and hydrophobic lines of 10 μm width. This particular pattern was adopted based on previous experiments with different pattern layouts, because it induced the greatest cellular alignment and nuclear elongation.[1] We plasma oxidized both groups under the same conditions, thus creating identical microtopography in both cases with grooves ~0.5 μm deep. Films from both groups were deposited on top of glass coverslips, thus we consider that the films have roughly the same stiffness. Therefore, the only changing parameter between thin and thick films is the level of hydrophobicity and any observed morphological differences between cultured cells are solely attributed to the corresponding difference in hydrophobicity.

There was no statistically significant difference in terms of alignment between cells seeded on thin (2 μm) and thick (10 μm) micropatterned Parylene C films. As shown before, the degree of alignment is a function of the oxygen plasma process conditions,[2] which further define the degree of the induced hydrophilicity and substrate microtopography.[21] While we have previously shown that Ca^{2+} cycling of NRVM on micropatterned Parylene C films is significantly improved compared to unstructured cultures,[2] in this study, we did not observe any significant changes in the Ca^{2+} transients of cells cultured on thin and thick micropatterned Parylene C substrates. Many studies have previously associated cellular alignment and sarcomeric organization with improved Ca^{2+} physiology of NRVM on structured tissue substrates.[11,25–27] These observations have been primarily attributed to changes in the sarcoplasmic reticulum organization[28] and voltage-gated Ca^{2+} currents.[3] Therefore, it is not surprising that Ca^{2+} handling parameters of NRVM were similar for cells cultured on both film thickness groups.

Although there was no difference in terms of Ca^{2+} cycling, there was a significant change in the way cells adhered to the micropatterned Parylene C substrates, which was quantified in terms of contact angles between the cells and the Parylene substrate at the level of the cellular nucleus. The lower hydrophobicity of thin films enabled the cardiomyocytes to bridge across these lines and attach to the neighboring hydrophilic lines, obtaining a more spread-out shape, whereas cells remained constrained on the hydrophilic lines on the thicker membranes and adopted a more cylindrical elongated shape.

NRVM on thin films had a significantly larger height and volume. As expected, when cells are less constrained by

boundaries (physical or other), they expand substantially in size. On the contrary, the natural hydrophobicity of the Parylene lines restricted the cells from expanding further, therefore cardiomyocytes on thick films were smaller in size (height and volume), but had a more elongated (*in vivo*-like) shape. The cylindrical and elongated cellular morphology observed on the 10 μm-thick-patterned Parylene C constructs is more representative of adult cardiomyocytes[29] and can potentially lead to more mature cells *in vitro*, but further morphological and physiological studies are required to conclude the level of cell maturation. These are also essential to elucidate whether the aforementioned observations are associated with the subcellular adult myocyte organization and function.

The change in NRVM morphology upon a change in Parylene film thickness was associated with changes in the cytoskeletal structure. Innately, microtubules of unstructured cells were significantly more spread out and sparsely distributed throughout the cytoplasm than structured cells, also reported by others.[30] The organization and increased microtubule density in cells on the micropatterned constructs are similar to that observed by others in adult rat cardiomyocytes.[30] Microtubule density was significantly ($p < 0.05$) higher in structured NRVMs on the thick micropatterned Parylene C films. This is most probably related to the cells' larger surface to volume ratio confirmed through the ion scanning microscopy measurements.

There are several possible reasons for this effect. One possibility is that the cells' larger surface to volume ratio influences cellular ultrastructure, as previously shown in myocytes where cell shape was manipulated.[31] A second possibility is that there is a different ECM deposition and characteristics on Parylene membranes of different thickness; this results in varied activation of cellular signalling pathways through transmembrane integrin-like mediators.[32] Finally, the degree of adhesion of cells on the substrate can differentially regulate mechanosensitive responses to cell contraction with consequent cytoskeletal rearrangement.[33] All these possibilities will be investigated in future experiments involving cell-cell interactions and measurements of contractility together with further assessment of signalling pathways involved in intercellular signalling.

Acknowledgments

This work was supported by the A.G. Leventis Foundation and the British Heart Foundation Cardiovascular Regenerative Medicine Centre RM/13/1/30157. The authors would like to thank Miss Karen Pinto for her assistance in cell culturing and Dr Patrizia Camelliti for her assistance in sarcomere immunofluorescent staining.

Disclosure Statement

No competing financial interests exist.

References

1. Rao, C., *et al.* The effect of microgrooved culture substrates on calcium cycling of cardiac myocytes derived from human induced pluripotent stem cells. Biomaterials **34,** 2399, 2013.
2. Trantidou, T., *et al.* Selective hydrophilic modification of Parylene C films: a new approach to cell micro-patterning for synthetic biology applications. Biofabrication **6,** 1, 2014.
3. Walsh, K.B., and Parks, G.E. Changes in cardiac myocyte morphology alter the properties of voltage-gated ion channels. Cardiovasc Res **55,** 64, 2002.
4. Bien, H., Yin, L., and Entcheva, E. Cardiac cell networks on elastic microgrooved scaffolds. IEEE Eng Med Biol Mag **22,** 108, 2003.
5. Bursac, N., Parker, K., Iravanian, S., and Tung, L. Cardiomyocyte cultures with controlled macroscopic anisotropy a model for functional electrophysiological studies of cardiac muscle. Circ Res **91,** e45, 2002.
6. Fast, V.G., and Kleberm A.G. Anisotropic conduction in monolayers of neonatal rat heart cells cultured on collagen substrate. Circ Res **75,** 591, 1994.
7. Rohr, S., Schölly, D., and Kleber, A.G. Patterned growth of neonatal rat heart cells in culture. Morphological and electrophysiological characterization. Circ Res **68,** 114, 1991.
8. Lieberman, M., Kootsey, J.M., Johnson, E.A., and Sawanobori, T. Slow conduction in cardiac muscle: a biophysical model. Biophys J **13,** 37, 1973.
9. De Diego, C., *et al.* Anisotropic conduction block and reentry in neonatal rat ventricular myocyte monolayers. Am J Physiol-Heart C **300,** H271, 2011.
10. Khademhosseini, A., *et al.* Microfluidic patterning for fabrication of contractile cardiac organoids. Biomed Microdevices **9,** 149, 2007.
11. Kim, D.H., *et al.* Nanoscale cues regulate the structure and function of macroscopic cardiac tissue constructs. PNAS **107,** 565, 2010.
12. Kai, D., Prabhakaran, M.P., Jin, G., and Ramakrishna, S. Guided orientation of cardiomyocytes on electrospun aligned nanofibers for cardiac tissue engineering. J Biomed Mater Res B **98**, 379, 2011.
13. Engelmayr G.C., *et al.* Accordion-like honeycombs for tissue engineering of cardiac anisotropy. Nat Mater **7,** 1003, 2008.
14. Trantidou, T, Humphrey, E.J., Kontziampasis, D., Terracciano, C., and Prodromakis, T. Biorealistic cardiac cell culture platforms with integrated monitoring of extracellular action potentials. Sci Rep **5**, 11067, 2015.
15. Iguchi, N., *et al.* Contact sensitivity to polychloroparaxylene-coated cardiac pacemaker, PACE **20,** 372–373, 1997.
16. Prodromakis, T., Michelakis, K., Zoumpoulidis, T., Dekker, R., and Toumazou, C. Biocompatible encapsulation of CMOS based chemical sensors. In IEEE Sensors, 2009, pp. 791–794.
17. Schmidt, E.M., McIntosh, J.S., and Bak, M.J. Long-term implants of Parylene-C coated microelectrodes. Med Biol Eng Comput **26,** 96, 1988.
18. Kahouli, A. Effect of film thickness on structural, morphology, dielectric and electrical properties of parylene c films. J Appl Phys **112,** 064103, 2012.
19. Huang, H., Xu, Y., and Low, H.Y. Effects of film thickness on moisture sorption, glass transition temperature and morphology of poly(chloro-para-xylylene) film. Polymer **46,** 5949, 2005.
20. Wei, L., Parhi, P., Vogler, E.A., Ritty, T.M., and Lakhtakia, A. Thickness-controlled hydrophobicity of fibrous parylene-c films. Mat Lett **64,** 1063, 2010.
21. Trantidou, T., Prodromakis, T., and Toumazou, C. Oxygen plasma induced hydrophilicity of Parylene- C thin films. Appl Surf Sci **261,** 43, 2012.

22. Korchev, Y.E., Bashford, C.L., Milovanovic, M., Vodyanoy, I., and Lab, M.J. Scanning ion conductance microscopy of living cells. Biophys J **73,** 653, 1997.
23. Novak, P., *et al*. Nanoscale live-cell imaging using hopping probe ion conductance microscopy. Nat Methods **6,** 279, 2009.
24. Chang, T.Y., *et al*. Cell and protein compatibility of parylene-c surfaces. Langmuir **23,** 11718, 2007.
25. Kaji, H., Takoh, K., Nishizawa, M., and Matsue, T. Intracellular Ca2+ imaging for micropatterned cardiac myocytes. Biotechnol Bioeng **81**, 748, 2003.
26. Feinberg, A.W., *et al*. Controlling the contractile strength of engineered cardiac muscle by hierarchal tissue architecture. Biomaterials **33**, 5732, 2012.
27. Yin, L., Bien, H., and Entcheva, E. Scaffold topography alters intracellular calcium dynamics in cultured cardiomyocyte networks. Am J Physiol Heart Circ Physiol **287,** H1276, 2004.
28. Shannon, T.R, Wang, F., and Bers, D.M. Regulation of cardiac sarcoplasmic reticulum Ca release by luminal [Ca] and altered gating assessed with a mathematical model. Biophys J **89,** 4096, 2005.
29. Yang, X., Pabon, L., and Murry, C.E. Engineering adolescence maturation of human pluripotent stem cell-derived cardiomyocytes. Circ Res **114,** 511, 2014.
30. Rothen-Rutishauser, B., Ehler, E., Perriard, E., Messerli, J., and Perriard, J. Different behaviour of the non-sarcomeric cytoskeleton in neonatal and adult rat cardiomyocytes. J Mol Cell Cardiol **30,** 19, 1998.
31. Kuo, P.L., *et al*. Myocyte shape regulates lateral registry of sarcomeres and contractility. Am J Pathol **181,** 2030, 2012.
32. Dabiri, B.E., Lee, H., and Parker, K.K. A potential role for integrin signaling in mechanoelectrical feedback. Prog Biophys Mol Biol **110,** 196, 2012.
33. McCain, M.L., and Parker, K.K. Mechanotransduction: the role of mechanical strew, myocyte shape, and cytoskeletal architecture on cardiac function. Pflugers Arch **462**, 89, 2011.

Address correspondence to:
Tatiana Trantidou, PhD
Department of Chemistry,
Imperial College London
Main Chemistry Building (34), Room 542
SW7 2AZ, London
United Kingdom

E-mail: t.trantidou@imperial.ac.uk

Cesare M. Terracciano, MD, PhD
National Heart and Lung Institute
ICTEM Building, Room 430
Imperial College London
Hammersmith Campus
W12 0NN, London
United Kingdom

E-mail: c.terracciano@imperial.ac.uk

Received: January 8, 2016
Accepted: March 11, 2016
Online Publication Date: April 20, 2016